electronic reprint

CRYSTALLOGRAPHIC COMMUNICATIONS

ISSN: 2056-9890

journals.iucr.org/e

# [*N*,*N*-Bis(2-hydroxyethyl)dithiocarbamato-$\kappa^2$*S*,*S*′]bis(triphenylphosphane-$\kappa$*P*)copper(I) chloroform monosolvate: crystal structure, Hirshfeld surface analysis and solution NMR measurements

**Sang Loon Tan, Chien Ing Yeo, Peter J. Heard, Geoffrey R. Akien, Nathan R. Halcovitch and Edward R. T. Tiekink**

*Acta Cryst.* (2016). E**72**, 1799–1805

Acta Cryst E CRYSTALLOGRAPHIC COMMUNICATIONS

ISSN 2056-9890

# [*N*,*N*-Bis(2-hydroxyethyl)dithiocarbamato-$\kappa^2 S,S'$]bis(triphenylphosphane-$\kappa P$)copper(I) chloroform monosolvate: crystal structure, Hirshfeld surface analysis and solution NMR measurements

Sang Loon Tan,[a] Chien Ing Yeo,[a] Peter J. Heard,[b] Geoffrey R. Akien,[c] Nathan R. Halcovitch[c] and Edward R. T. Tiekink[a]*

[a]Research Centre for Crystalline Materials, Faculty of Science and Technology, Sunway University, 47500 Bandar Sunway, Selangor Darul Ehsan, Malaysia, [b]Office of the Provost, Sunway University, 47500 Bandar Sunway, Selangor Darul Ehsan, Malaysia, and [c]Department of Chemistry, Lancaster University, Lancaster LA1 4YB, UK. *Correspondence e-mail: edwardt@sunway.edu.my

Received 3 November 2016
Accepted 7 November 2016

Edited by W. T. A. Harrison, University of Aberdeen, Scotland

**Keywords:** crystal structure; copper; dithiocarbamate; hydrogen bonding; Hirshfeld surface analysis; NMR.

**CCDC reference**: 1515483

**Supporting information**: this article has supporting information at journals.iucr.org/e

The title compound, $[Cu(C_5H_5NO_2S_2)(C_{18}H_{15}P)_2]\cdot CHCl_3$, features a tetrahedrally coordinated $Cu^I$ atom within a $P_2S_2$ donor set defined by two phosphane P atoms and by two S atoms derived from a symmetrically coordinating dithiocarbamate ligand. Both intra- and intermolecular hydroxy-O—H···O(hydroxy) hydrogen bonding is observed: the former closes an eight-membered $\{\cdots HOC_2NC_2O\}$ ring, whereas the latter connects centrosymmetrically related molecules into dimeric aggregates *via* eight-membered $\{\cdots H—O\cdots H—O\}_2$ synthons. The complex molecules are arranged to form channels along the *c* axis in which reside the chloroform molecules, being connected by Cl···$\pi$(arene) and short S···Cl [3.3488 (9) Å] interactions. The intermolecular interactions have been investigated further by Hirshfeld surface analysis, which shows the conventional hydrogen bonding to be very localized with the main contributors to the surface, at nearly 60%, being H···H contacts. Solution NMR studies indicate that whilst the same basic molecular structure is retained in solution, the triphenylphosphane ligands are highly labile, exchanging rapidly with free $Ph_3P$ at room temperature.

## 1. Chemical context

The motivation to prepare bis(phosphane)copper(I) dithiocarbamates of general formula $(R_3P)_2Cu(S_2CNR'R'')$ (*R*, *R*′, *R*″ = alkyl, aryl) largely stems from the versatile biological properties exhibited by these types of compounds (Skrott & Cvek, 2012; Biersack *et al.*, 2012) and metal dithiocarbamates in general, as summarized in a recent review (Hogarth, 2012). At present, research continues to develop promising anti-microbial agents in light of the growing prevalence of bacterial infections and threats associated with drug-resistant bacteria (Verma & Singh, 2015; Onwudiwe *et al.*, 2016). In our recent efforts to develop anti-microbial agents, phosphanegold(I) dithiocarbamates, $R_3PAu[S_2CN(iPr)CH_2CH_2OH]$, were prepared and these compounds demonstrated prominent and distinctive anti-microbial activity against a broad range of Gram-positive and Gram-negative bacteria, dependent on the type of P-bound substituent employed (Sim *et al.*, 2014). A distinct structure–activity relationship was noted in that when *R* = Et, the compound was potent against a broad range of Gram-positive and Gram-negative bacteria, whereas the *R* = Ph and Cy compounds showed specific activity against Gram-

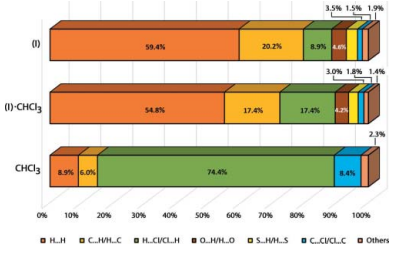

positive bacteria. Even greater, broad-range activity is apparent in triethylphosphanegold(I) dialkyldithiocarbamates (Chen *et al.*, 2016). The above prompted an exploration of the anti-bacterial activity of related copper(I) and silver(I) derivatives, as these metals are known to possess noteworthy potential as anti-microbial agents (Losasso *et al.*, 2014). Thus, a series of phosphanecopper(I) and silver(I) compounds of general formula $(Ph_3P)_2M[S_2CN(R)CH_2CH_2OH]$ for $M$ = Cu and Ag, and $R$ = Me, *i*Pr and $CH_2CH_2OH$, were prepared and evaluated for their anti-microbial activities (Jamaludin *et al.*, 2016). While none of the studied compounds exhibited activity against Gram-negative bacteria, they were found to be selectively potent against Gram-positive bacteria. Following new syntheses to evaluate further the potential of this class of compounds, crystals became available for the title complex, $(Ph_3P)_2Cu[S_2CN(CH_2CH_2OH)_2]$ (I), as its 1:1 chloroform solvate. Herein, the crystal and molecular structures of (I)·$CHCl_3$ are described along with an analysis of its Hirshfeld surface. Finally, some non-standard, *e.g.* variable temperature, NMR measurements are presented in order to gain insight into the solution structure.

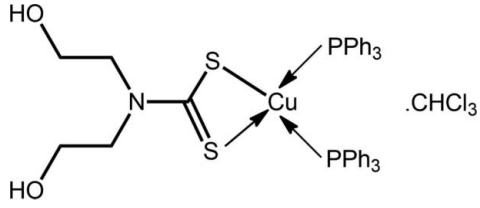


## 2. Structural commentary

The molecular structure of the complex in (I)·$CHCl_3$ is shown in Fig. 1 and selected geometric parameters are collected in Table 1. The copper atom is bound by two dithiocarbamate-S atoms and two phosphane-P atoms. The dithiocarbamate ligand is coordinating in a symmetric mode with Δ(Cu—S) = 0.042 Å, being the difference between the Cu—$S_{long}$ and Cu—$S_{short}$ bond lengths. This near equivalence in Cu—S bond lengths is reflected in the experimental equivalence of the associated C1—S1, S2 bond lengths. A small disparity, *i.e.* 0.02 Å, is noted in the Cu—P bond lengths. The resulting $P_2S_2$ donor set defines an approximate tetrahedral geometry. A measure of tetrahedral *vs* square-planar geometry is the value of $\tau_4$ (Yang *et al.*, 2007) with values of 1.0 and 0.0° corresponding to ideal tetrahedral and square planar geometries, respectively. In the case of the complex in (I)·$CHCl_3$, the value computes to 0.80. Distortions from the ideal tetrahedral

**Table 1**
Geometric data (Å, °) for (I) in (I)·$CHCl_3$ and (I) in its 1:1 $Ph_3P$ co-crystal.

| Parameter | (I) in (I)·$CHCl_3$ | (I) in (I)·$PPh_3$[a] |
|---|---|---|
| Cu—S1 | 2.3791 (6) | 2.3948 (12) |
| Cu—S2 | 2.4213 (5) | 2.4288 (12) |
| Cu—P1 | 2.2602 (6) | 2.2849 (12) |
| Cu—P2 | 2.2380 (5) | 2.2594 (12) |
| C1—S1 | 1.714 (2) | 1.709 (4) |
| C1—S2 | 1.717 (2) | 1.702 (4) |
| S1—Cu—S2 | 75.264 (18) | 74.76 (4) |
| S1—Cu—P1 | 110.96 (2) | 109.85 (5) |
| S1—Cu—P2 | 109.81 (2) | 112.35 (4) |
| S2—Cu—P1 | 103.74 (2) | 102.50 (4) |
| S2—Cu—P2 | 123.17 (2) | 122.04 (5) |
| P1—Cu—P2 | 123.65 (2) | 124.52 (4) |

Note: (*a*) Jian *et al.* (2000).

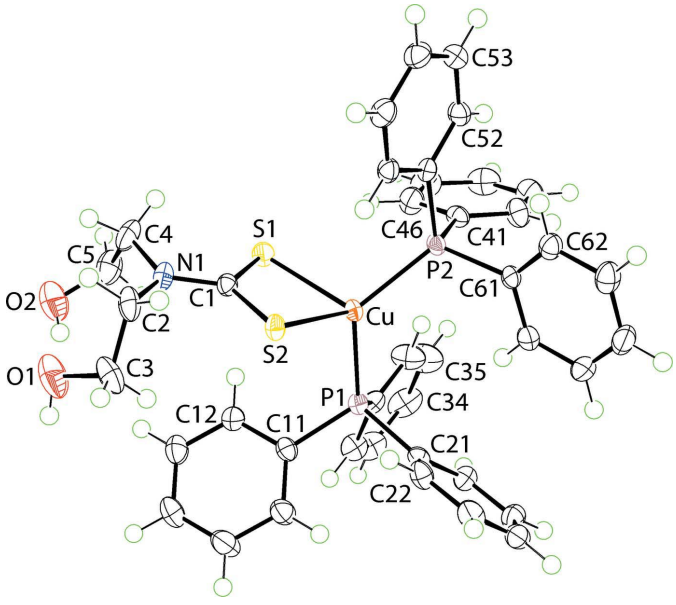


**Figure 1**
The molecular structure of the complex in (I)·$CHCl_3$, showing the atom-labelling scheme and displacement ellipsoids at the 70% probability level. The solvent $CHCl_3$ molecule is omitted.

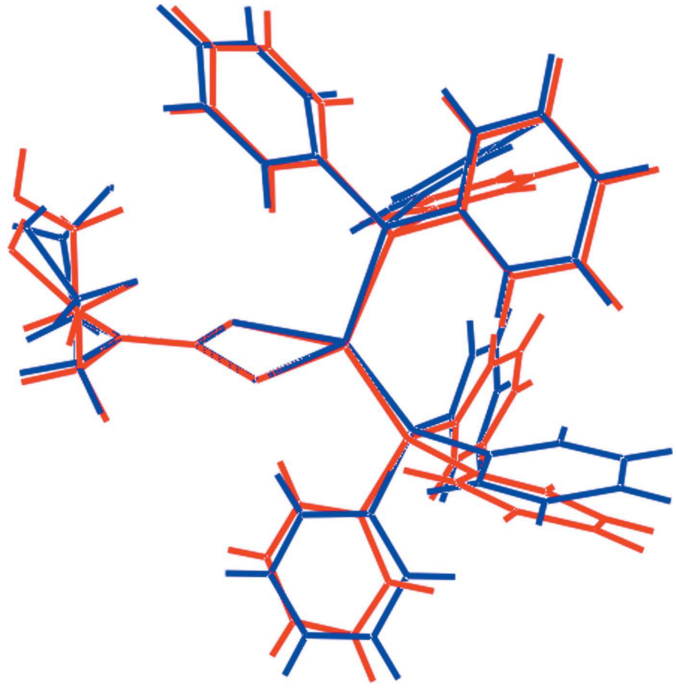

**Figure 2**
Overlay diagram of (I)·$CHCl_3$ (red image) and (I)·$Ph_3P$ (blue). The molecules have been overlapped so the chelate rings are coincident. The $CHCl_3$ and $Ph_3P$ molecules have been omitted.

**Table 2**
Hydrogen-bond geometry (Å, °).

*Cg*1 is the ring centroid of (C51–C56).

| *D*—H···*A* | *D*—H | H···*A* | *D*···*A* | *D*—H···*A* |
|---|---|---|---|---|
| O2—H2*O*···O1 | 0.84 | 1.95 | 2.710 (3) | 150 |
| O1—H1*O*···O2$^{i}$ | 0.86 | 1.97 | 2.697 (3) | 142 |
| C6—Cl3···*Cg*1 | 1.77 (1) | 3.81 (1) | 3.798 (3) | 76 (1) |

Symmetry code: (i) $-x, -y+2, -z+2$.

geometry are clearly related to the acute angle subtended by the dithiocarbamate ligand and the wide angle subtended by the bulky triphenylphosphane ligands, Table 1.

The structure of (I) has also been determined in its 1:1 co-crystal with $PPh_3$ (Jian *et al.*, 2000), hereafter (I)·$Ph_3P$, and key geometric parameters for this structure are also included in Table 1. Interestingly, within pairs of comparable bond lengths, those in (I)·$PPh_3$ are systematically longer. However, the value of $\Delta$(Cu—S) is slightly less at 0.034 Å. The value of $\tau_4$ is identical at 0.80. An overlay diagram for (I) in each of (I)·$CHCl_3$ and (I)·$PPh_3$ is shown in Fig. 2 which confirms the very similar conformations adopted for (I) in both structures.

## 3. Supramolecular features

Geometric parameters describing the salient intermolecular interactions in the crystal of (I)·$CHCl_3$ are collated in Table 2. There are two types of hydroxy-O—H···O(hydroxy) hydrogen bonding in the molecular packing, one intramolecular and the other intermolecular. The former has hydroxy-O2—H as the donor and the hydroxy-O1 as the acceptor, and closes an eight-membered {···$HOC_2NC_2O$} ring. The key feature of the molecular packing is the presence of hydroxy-O—H···O(hydroxy) hydrogen bonding which connects centrosymmetricly-related molecules into dimeric aggregates *via* eight-membered {···H—O···H—O}$_2$ synthons, encompassing the intramolecular hydroxy-O—H···O(hydroxy) hydrogen bonds, Fig. 3*a*. The only other identifiable directional interactions within standard distance criteria (Spek, 2009) involve the chloroform molecule. Thus, a chloroform-Cl3···$\pi$(arene) interaction is noted, Table 2. In addition, there is evidence for a close S1···Cl3 contact, *i.e.* involving the same chlorine atom as in the just mentioned Cl···$\pi$(arene) interaction. The separation of 3.3488 (9) Å is about 0.2 Å less than the sum of their van der Waals radii (Spek, 2009). In a very recent and exhaustive review of halogen bonding (Cavallo *et al.*, 2016), it was mentioned that sulfur is well known to function as an acceptor in *R*—*X*···S synthons. The interactions involving the chloroform molecule are highlighted in Fig. 3*b*. Globally, molecules of the copper(I) complex pack to define channels parallel to the *c* axis in which reside the solvent molecules, Fig. 3*c*. Given the presence of $Ph_3P$ ligands in (I)·$CHCl_3$, evidence was sought for phenyl-embraces (Dance & Scudder, 1995). While none was apparent for the P1-phosphane, centrosymmetrically related P2-phosphane ligands approach each other in this manner to generate a sixfold phenyl-embrace. The closest interactions between the phosphane residues in this embrace is a pair of edge-to-face-phenyl—H···$\pi$(arene) interactions, *i.e.* C63—H63···$\pi$(C51–C56)$^{i}$ = 3.25 Å with an angle at H62 of 133°; symmetry operation (i): $1-x, 1-y, 1-z$.

## 4. Hirshfeld surface analysis

The protocols for the Hirshfeld surface analysis were as described recently (Yeo *et al.*, 2016). In the present study, analyses were conducted on the following three species: (I) in (I)·$CHCl_3$, (I)·$CHCl_3$ and $CHCl_3$ alone. Hirshfeld surface

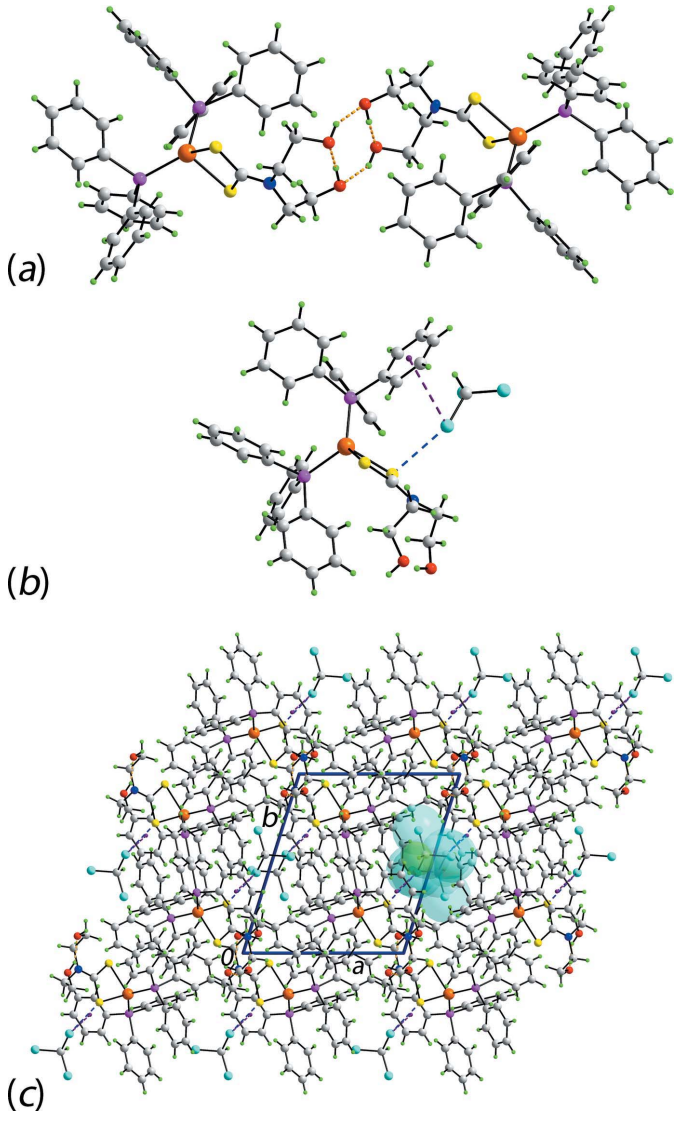


**Figure 3**
Molecular packing in (I)·$CHCl_3$: (*a*) supramolecular dimer sustained by hydroxy-O—H···O(hydroxy) hydrogen bonding shown as orange dashed lines, (*b*) a view of the interactions between the complex and solvent molecules with the Cl···$\pi$(arene) and Cl···S interactions shown as purple and blue dashed lines, respectively, and (*c*) a view of the unit-cell contents in projection down the *c* axis, with chloroform molecules occupying one channel highlighted in space-filling mode.

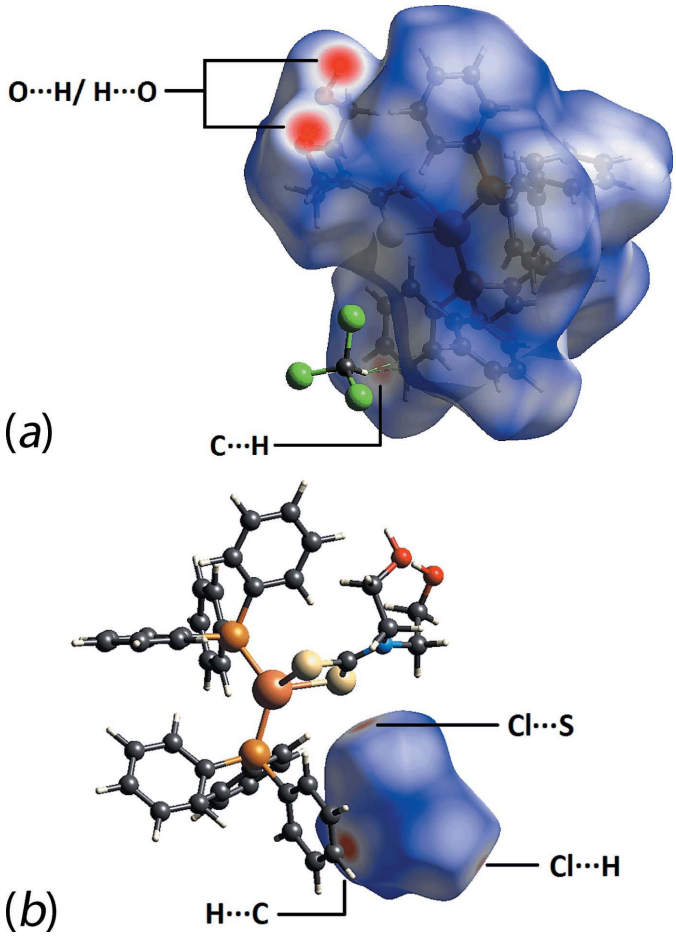


**Figure 4**
Comparison of the Hirshfeld surfaces of (*a*) molecule (I) in (I)·$CHCl_3$ and (*b*) $CHCl_3$ in (I)·$CHCl_3$, highlighting intermolecular interactions formed with the other component of the structure. The Hirshfeld surfaces were mapped over $d_{norm}$ within the range −0.572 to 1.457 Å.

analysis provides visualization on the existence of any intermolecular interactions within close proximity in a crystal structure, for which contact distances shorter than the sum of the respective van der Waals radii appear red while at distances equal or longer than this would be white and blue in appearance, respectively. Figs. 4*a* and *b* show Hirshfeld surfaces mapped over $d_{norm}$ for (I) and $CHCl_3$, respectively. The former image exhibits intense red spots on the surface near the hydroxyethyl substituents which are correlated with the strong O—H···O hydrogen bonding. Apart from these dominant interactions, several other red spots attributed to the close contacts between the complex and chloroform molecules, *i.e.* C···H/H···C, S···Cl/Cl···S and H···Cl/Cl···H, are evident in Fig. 4*a* and *b*.

The combination of $d_i$ and $d_e$ distances resulted in two-dimensional cuttlefish- and chicken wing-like fingerprint plots for (I), (I)·$CHCl_3$ and $CHCl_3$, Fig. 5*a*, which may be decomposed into several essential close contacts as shown in Fig. 5*b*–*d*. In general, complex (I) and its chloroform solvate exhibit almost identical profiles except that the pincer form of (I) in its decomposed fingerprint plot delineated into C···H/H···C contacts shows two different tips at $d_e + d_i \sim 2.5$ Å and ∼2.7Å in contrast to the pincer form of (I)·$CHCl_3$ with a pair of symmetrical tips at $d_e + d_i \sim 2.7$ Å when the solvate is considered as a single entity. The close contact distance ($d_e + d_i \sim 2.5$ Å), which is shorter than the sum of van der Waals radii of 2.9 Å (Spek, 2009), is also reflected in the lancet blade-like fingerprint plot of the solvent molecule corresponding to the Cl—H···C($\pi$) interaction. The H···Cl/Cl···H contact, on the other hand, contributes to the half-pincer form in the decomposed fingerprint plot of (I) and develops into the full pincer form in (I)·$CHCl_3$, both with $d_e + d_i \sim 2.9$ Å that is very close to the sum of van der Waals radii (2.95 Å). As expected, O···H/H···O contacts constitute the strongest among all interactions with $d_e + d_i \sim 1.9$ Å (*cf.* the sum of van der Waals radii of 2.75 Å) in the forceps form of both decomposed fingerprint plots of (I) and (I)·$CHCl_3$, Fig. 5*d*. Based on the asymmetric fingerprint patterns of the C···H/H···C and Cl···H/H···Cl contacts, Fig. 5*b* and *c*, and the symmetric pattern of the O···H/H···O contacts, Fig. 5*d*, it may be concluded that two complex molecules are very closely associated, as shown in Fig. 3*a*, and these are flanked by two $CHCl_3$ molecules, highlighted in Fig. 3*b*.

The quantification on the distribution of each of the contacts to the Hirshfeld surface reveals that H···H, C···H/H···C and H···Cl/Cl···H are the three main components for

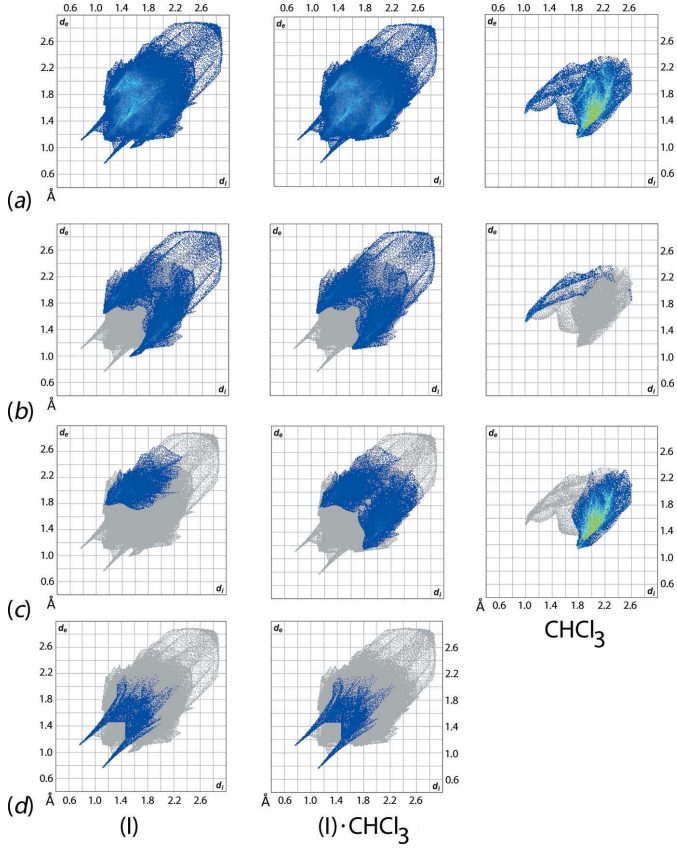


**Figure 5**
Comparison between (I) in (I)·$CHCl_3$, (I)·$CHCl_3$ and $CHCl_3$ of the (*a*) full two-dimensional fingerprint plots, and the plots delineated into (*b*) C···H/H···C, (*c*) Cl···H/H···Cl and (*d*) O···H/H···O contacts.

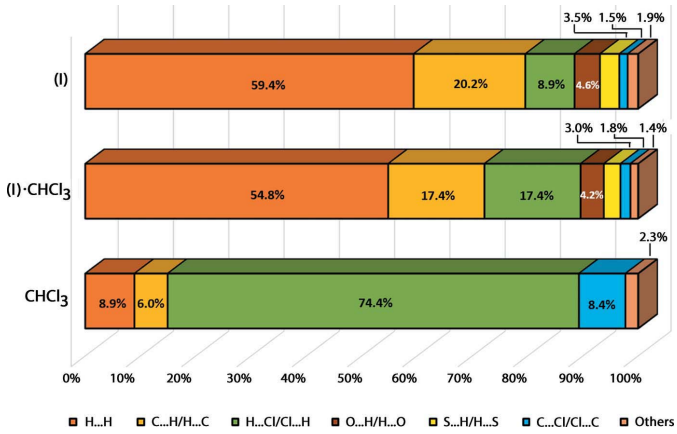


**Figure 6**
Percentage contributions of the different close contacts to the Hirshfeld surface of (I) in (I)·$CHCl_3$, (I)·$CHCl_3$ and $CHCl_3$.

(I) in (I)·$CHCl_3$, with the corresponding contributions of *ca* 59.4, 20.2 and 8.9%, respectively, Fig. 6. Despite this, not all of these contacts result in meaningful interactions based on the comparison between $d_e + d_i$ contact distances and the sum of the van der Waals radii. This sequence is followed by O···H/H···O contacts which form the fourth most dominant interactions with a contribution of approximately 4.6% to the overall Hirshfeld surface. In general, there is not much deviation of the topological distribution between (I) and (I)·$CHCl_3$ except that the contribution from H···Cl/Cl···H increases by nearly twofold upon the inclusion of the solvent molecule in (I)·$CHCl_3$. As for the chloroform molecule, H···Cl/Cl···H makes the major contribution at 74.4%, followed by 8.9% from H···H and 8.4% from H···Cl/Cl···H; the remaining contributions from other minor contacts.

As mentioned previously, Cl···$\pi$(arene) and S···Cl interactions are formed by the chloroform molecule. In order to gain insight into the charge distribution and rationalize these close contacts, the electrostatic potential (ESP) was mapped over the Hirshfeld surface by *ab initio* Hartree–Fock (HF) quantum modelling with the 6-31G(d) basis set, as this represents the best possible level of theory and basis set functions in this study so as to keep the accuracy and computational cost at manageable level.

As shown in Fig. 7*a*, a phenyl ring of the complex molecule exhibits mild electronegative character as evidenced from the pale-red spot on the ESP map in contrast to the strong electropositive character about $CHCl_3$, being intense-blue. The electropositive character of the methine group extends slightly beyond the chloro atom approaching its equatorial ring of the negative charge region, hence establishing the weak Cl···$\pi$(arene) interaction with $d_e + d_i \sim 3.3$ Å being slightly less than the sum of van der Waals radii of 3.45 Å. The S···Cl halogen bond, on the other hand, is established through the highly directional interaction between the electronegative sulfur of (I) and the $\sigma$-hole of the chloro atom of $CHCl_3$ with weak electropositive character, Fig. 7*b*. The electropositive character of the $\sigma$-hole results from the electron deficiency in the outer lobe of the *p* orbital (non-bonded) when a half-filled *p* orbital of a halogen participates in the formation of covalent bond (Clark *et al.*, 2007).

## 5. NMR Study

FT NMR spectra were recorded on a Bruker AVANCE III 400 MHz spectrometer, operating at 400.13, 100.61 and 161.98 MHz, respectively, for $^1$H, $^{13}$C and $^{31}$P. Spectra were indirectly referenced to the solvent deuterium lock shift; chemical shifts are quoted relative to TMS and 85% $H_3PO_4$. Probe temperatures were controlled by a standard variable temperature unit and are considered accurate to within ±1 K. Spectra were acquired on approximately 14 mmol solutions of (I) in each of $CD_2Cl_2$, $d_6$-DMSO and $CDCl_2CDCl_2$.

The ambient temperature (298 K) $^1$H NMR spectra of (I) display the expected signals due to the triphenylphosphine and dithiocarbamate ligands. The spectra are qualitatively identical in all three solvents, with the only significant differences being the position of the –OH signal of the dithiocarbamate ligand.

The aromatic region of the $^1$H spectrum in $d_6$-DMSO shows two multiplets at *ca* 7.39 ppm (6 H) and 7.28 ppm (24 H) attributable to Ph-H atoms of the triphenylphosphine ligands. A sharp singlet observed at 8.32 ppm (1 H) was assigned to

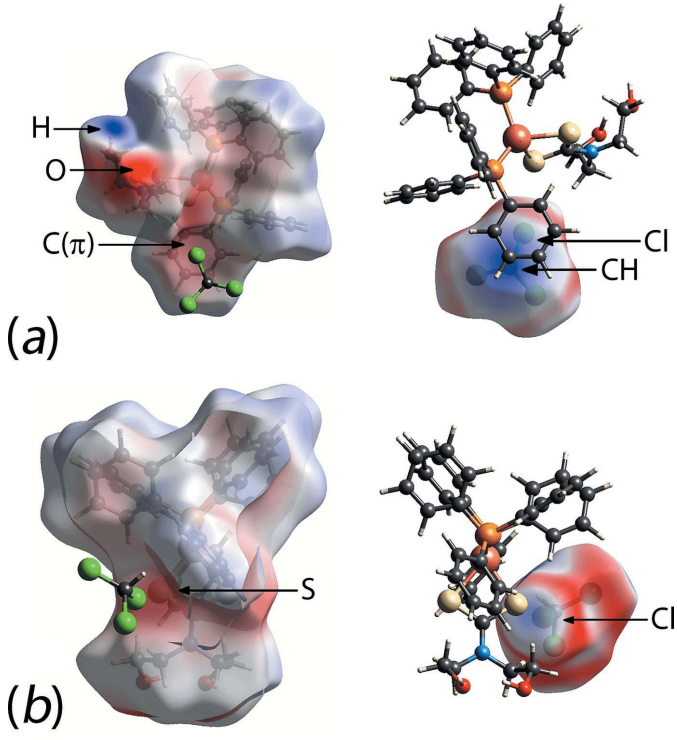


**Figure 7**
Electrostatic potential (ESP) mapped over the Hirshfeld surfaces of the complex molecule (I) (left) and $CHCl_3$ (right), showing the attraction between the electronegative (red) and electropositive (blue) sites for (*a*) Cl···$\pi$(arene) and (*b*) S···Cl interactions, respectively. The ESP was mapped onto the Hirshfeld surface within the isocharge value of −0.119 to 0.164 a.u. by the *ab initio* Hartree–Fock (HF) quantum modelling approach with the 6-31G(d) basis set.

$CHCl_3$, as seen in the X-ray crystal structure analysis. The dithiocarbamate moiety displays a single set of resonances, indicating the two $–CH_2CH_2OH$ groups are chemically equivalent. The –OH groups display a triplet at 4.80 ppm ($^3J_{HH}$ = 5.3 Hz), which disappears on the addition of $D_2O$. The methylene hydrogen atoms display a triplet at 3.96 ppm ($^3J_{HH}$ = 6.4 Hz) and a pseudo quartet at 3.65 ppm, assignable to $NCH_2$– and $–CH_2OH$, respectively. On the addition of $D_2O$, the quartet collapses to a triplet.

The $^{13}C\{^1H\}$ spectra in each of the solvents are also qualitatively identical. In $d_6$-DMSO solution, the carbon atoms of the triphenylphospine ligands give rise to four resonances at 134.6 ppm (very weak, *d*, $^1J_{PC}$ ~22 Hz, $C_{ipso}$), 133.6 ppm (*d*, $^2J_{PC}$ = 12 Hz, $C_{ortho}$), 130.1 ppm (*s*, $C_{para}$) and 128.9 ppm (*d*, $^3J_{PC}$ = 5.70 Hz, $C_{meta}$). The dithiocarbamate ligand shows two signals due to the methylene carbon atoms at 58.7 ppm ($NCH_2$—) and 56.0 ppm (—$CH_2OH$), respectively. The quaternary carbon atom of the dithiocarbamate was not observed.

The ambient temperature $^{31}P\{^1H\}$ spectrum in $CD_2Cl_2$ displays as single, broad resonance at −1.55 ppm ($\Delta\nu_{1/2}$ = 280 Hz). The line broadening is attributed to rapid relaxation of Cu *via* the quadrupole relaxation (QR) mechanism. Quadrupole relaxation is strongly temperature dependent: the rate of relaxation increases as the temperature decreases. On cooling, the signal sharpens progressively: $\Delta\nu_{1/2}$ (203 K) ~35 Hz. The sharpening presumably arises because of the effective 'decoupling' of the $^{65}Cu$–$^{31}P$ and $^{63}Cu$–$^{31}P$ scalar couplings as the rate of (Cu) relaxation increases (Grace *et al.*, 1970). The addition of *ca* 2 mg (0.9 equivalents) of triphenylphosphine at ambient temperature, to putatively give (I)·$PPh_3$, gives a single, broad peak at *ca* −3 ppm, which is between the chemical shifts of pure (I) and free $PPh_3$ (*ca* −6 ppm), indicating rapid exchange of the triphenylphosphine ligands.

In an attempt to resolve the Cu-P *J* couplings, $^{31}P\{^1H\}$ spectra were recorded in $CDCl_2CDCl_2$ solution at elevated temperatures (to reduce the rate of QR). However, no significant changes were observed in the line widths on elevating the temperature to 328 K, and any Cu–P coupling, if not lost through reversible ligand dissociation, remained unresolved. There was no evidence of decomposition at higher temperatures in this solvent.

There are two key conclusions from the foregoing. Firstly, the experiments with $D_2O$ proving exchange of the hydroxy-H atom indicates that this atom is labile, suggesting functionalization at this group should, in principle, be feasible. Secondly, the presence of additional $Ph_3P$ in solution does not result in displacement of the dithiocarbamate ligand nor force a monodentate mode of coordination proving the stability of complex (I) in each of (I)·$CHCl_3$ and (I)·$PPh_3$, and in solution.

## 6. Database survey

The structural chemistry of $(R_3P)_2Cu(S_2CNR'R'')$ compounds was summarized very recently (Jamaludin *et al.*, 2016). In all, there are eight examples now available in the literature, namely $\{(Ph_3P)_2Cu[S_2CN(Me)(CH_2CH_2OH)]\}\cdot CH_2Cl_2$ Jamaludin *et al.*, 2016), $[(Ph_3P)_2Cu\{S_2CN(CH_2CH_2OH)_2\}]\cdot PPh_3$ (Jian *et al.*, 2000), $[(Ph_3P)_2Cu\{S_2CN(n\text{-}Pr)_2\}]\cdot CH_2Cl_2$ (Xu *et al.*, 2001), $[(Ph_3P)_2Cu\{S_2CN(CH_2CH_2)_2S\}]\cdot CH_2Cl_2$ (Gupta *et al.*, 2013), $[(Ph_3P)_2Cu\{S_2CN(CH_2CH_2)_2NPh\}]$ (Gupta *et al.*, 2013), $[(Ph_3P)_2Cu\{S_2CN(Me)CH_2Ph\}]\cdot CH_2Cl_2$ (Kumar *et al.*, 2009) and $[(Ph_3P)_2Cu\{S_2CN(CH_2Ph)(CH_2py\text{-}4)\}]\cdot 2H_2O$ (Rajput *et al.*, 2012). Interestingly, all but one structure co-crystallizes with another molecule, solvent or otherwise, perhaps indicating inefficient molecular packing for these molecules. The $P_2S_2$ donor sets all eight compounds approximate tetrahedral angles with the range of $\tau_4$ values being a low 0.78 in $\{(Ph_3P)_2Cu[S_2CN(Me)(CH_2CH_2OH)]\}\cdot CH_2Cl_2$ (Jamaludin *et al.*, 2016) to a high of 0.85 in $[(Ph_3P)_2Cu\{S_2CN(CH_2CH_2)_2S\}]\cdot CH_2Cl_2$ (Gupta *et al.*, 2013), the narrow range emphasizing the similarity in the molecular structures/geometries.

## 7. Synthesis and crystallization

All chemicals and solvents were used as purchased without purification, and all reactions were carried out under ambient conditions. The melting point was determined on a Biobase automatic melting point apparatus MP450. The IR spectrum was obtained on a Perkin Elmer Spectrum 400 FT Mid-IR/Far-IR spectrophotometer from 4000 to 400 $cm^{-1}$; abbreviations: *br*, broad; *m*, medium; *s*, strong.

Preparation of (I)·$CHCl_3$: triphenylphosphine (Alfa Aesar, 2 mmol, 0.524 g) in acetonitrile (Merck, 10 ml) was added to copper(I) chloride (Sigma Aldrich, 1 mmol, 0.099 g) in acetonitrile (10 ml), followed by addition of a dispersion of potassium bis(2-hydroxyethyl)dithiocarbamate (1 mmol, 0.219 g) in acetonitrile (15 ml), prepared from the standard procedures (Jamaludin *et al.*, 2016). The resulting mixture was stirred for 2 h at room temperature. Chloroform (Merck, 35 ml) was added to the reaction mixture and it was left for slow evaporation at room temperature. Yellow blocks of (I)·$CHCl_3$ were obtained after one day. Yield: 0.699 g (91%). M.p. 423.8–424.5 K. IR ($cm^{-1}$): 3268 (*br*) (OH), 1433 (*s*) (C—N), 1168 (*m*), 990 (*s*) (C—S).

## 8. Refinement

Crystal data, data collection and structure refinement details are summarized in Table 3. Carbon-bound H atoms were placed in calculated positions (C—H = 0.95–1.00 Å) and were included in the refinement in the riding-model approximation, with $U_{iso}$(H) set to $1.2U_{eq}$(C). Refinement of the O-bound H atoms proved unstable so these atoms were fixed in the model in the positions revealed by a difference Fourier map, with $U_{iso}$(H) = $1.5U_{eq}$(O). The maximum and minimum residual electron density peaks of 1.97 and 1.93 e $Å^{-3}$, respectively, were located 0.78 and 0.62 Å from the Cl1 atom. While this feature of the difference map might indicate disorder, additional peaks that might be anticipated for the other atoms in the disordered component of chloroform molecule were not evident. This, plus the observation that the anisotropic displacement parameters of the atoms comprising the

chloroform molecule exhibited no unusual features, suggest the residual electron densities have limited chemical significance. Finally, owing to poor agreement, four reflections, *i.e.* (326), (1$\bar{1}$5), (666) and (1$\bar{4}$2) , were omitted from the final cycles of refinement.


## Acknowledgements

We thank Sunway University for support of biological and crystal engineering studies of metal dithiocarbamates.


## References


Biersack, B., Ahmad, A., Sarkar, F. H. & Schobert, R. (2012). *Curr. Med. Chem.* **19**, 3949–3956.

Brandenburg, K. (2006). *DIAMOND*. Crystal Impact GbR, Bonn, Germany.

Cavallo, G., Metrangolo, P., Milani, R., Pilati, T., Priimagi, A., Resnati, G. & Terraneo, G. (2016). *Chem. Rev.* **116**, 2478–2601.

Chen, B.-J., Jamaludin, N. S., Khoo, C.-H., See, T.-H., Sim, J.-H., Cheah, Y.-K., Halim, S. N. A., Seng, H.-L. & Tiekink, E. R. T. (2016). *J. Inorg. Biochem.* **163**, 68–80.

Clark, T., Hennemann, M., Murray, J. S. & Politzer, P. (2007). *J. Mol. Model.* **13**, 291–296.

Dance, I. & Scudder, M. (1995). *J. Chem. Soc. Chem. Commun*. pp. 1039–1040.

Farrugia, L. J. (2012). *J. Appl. Cryst.* **45**, 849–854.

Gans, J. & Shalloway, D. (2001). *J. Mol. Graphics Modell.* **19**, 557–559.

Grace, M., Beall, H. & Bushweller, C. H. (1970). *J. Chem. Soc. D*, p. 701.

Gupta, A. N., Singh, V., Kumar, V., Rajput, A., Singh, L., Drew, M. G. B. & Singh, N. (2013). *Inorg. Chim. Acta*, **408**, 145–151.

Hogarth, G. (2012). *Mini Rev. Med. Chem.* **12**, 1202–1215.

Jamaludin, N. S., Halim, S. N. A., Khoo, C.-H., Chen, B.-J., See, T.-H., Sim, J.-H., Cheah, Y.-K., Seng, H.-L. & Tiekink, E. R. T. (2016). *Z. Kristallogr*. **231**, 341–349.

Jian, F.-F., Bei, F.-L., Lu, L.-D., Yang, X.-J., Wang, X., Razak, I. A., Shanmuga Sundara Raj, S. & Fun, H.-K. (2000). *Acta Cryst.* C**56**, e288–e289.

Kumar, A., Mayer-Figge, H., Sheldrick, W. S. & Singh, N. (2009). *Eur. J. Inorg. Chem*. pp. 2720–2725.

Losasso, C., Belluco, S., Cibin, V., Zavagnin, P., Mičetić, I., Gallocchio, F., Zanella, M., Bregoli, L., Biancotto, G. & Ricci, A. (2014). *Front. Microbiol*. **5**, 1–9.

Onwudiwe, D. C., Ekennia, A. C. & Hosten, E. (2016). *J. Coord. Chem.* **69**, 2454–2468.

Rajput, G., Singh, V., Singh, S. K., Prasad, L. B., Drew, M. G. B. & Singh, N. (2012). *Eur. J. Inorg. Chem*. pp. 3885–3891.

Rigaku Oxford Diffraction (2015). *CrysAlis PRO*. Agilent Technologies Inc., Santa Clara, CA, USA.

Sheldrick, G. M. (2008). *Acta Cryst.* A**64**, 112–122.


**Table 3**
Experimental details.

| | |
|---|---|
| Crystal data | |
| Chemical formula | $[Cu(C_5H_5NO_2S_2)(C_{18}H_{15}P)_2]\cdot CHCl_3$ |
| $M_r$ | 887.71 |
| Crystal system, space group | Triclinic, $P\bar{1}$ |
| Temperature (K) | 100 |
| $a, b, c$ (Å) | 10.7271 (2), 13.5412 (2), 15.9361 (3) |
| $\alpha, \beta, \gamma$ (°) | 67.747 (2), 87.126 (2), 72.826 (2) |
| $V$ (Å$^3$) | 2041.92 (7) |
| $Z$ | 2 |
| Radiation type | Mo $K\alpha$ |
| $\mu$ (mm$^{-1}$) | 0.95 |
| Crystal size (mm) | 0.44 × 0.24 × 0.19 |
| | |
| Data collection | |
| Diffractometer | Rigaku SuperNova, Dual Mo at zero, AtlasS2 |
| Absorption correction | Multi-scan (*CrysAlis PRO*; Rigaku Oxford Diffraction, 2015) |
| $T_{min}$, $T_{max}$ | 0.928, 1.000 |
| No. of measured, independent and observed [$I > 2\sigma(I)$] reflections | 78295, 11363, 10195 |
| $R_{int}$ | 0.029 |
| $(\sin\theta/\lambda)_{max}$ (Å$^{-1}$) | 0.708 |
| | |
| Refinement | |
| $R[F^2 > 2\sigma(F^2)]$, $wR(F^2)$, $S$ | 0.045, 0.117, 1.03 |
| No. of reflections | 11363 |
| No. of parameters | 478 |
| H-atom treatment | H-atom parameters constrained |
| $\Delta\rho_{max}$, $\Delta\rho_{min}$ (e Å$^{-3}$) | 1.97, −1.93 |

Computer programs: *CrysAlis PRO* (Rigaku Oxford Diffraction, 2015), *SHELXS* (Sheldrick, 2008), *SHELXL2014* (Sheldrick, 2015), *ORTEP-3 for Windows* (Farrugia, 2012), *QMol* (Gans & Shalloway, 2001), *DIAMOND* (Brandenburg, 2006) and *publCIF* (Westrip, 2010).


Sheldrick, G. M. (2015). *Acta Cryst.* C**71**, 3–8.

Sim, J. H., Jamaludin, N. S., Khoo, C. H., Cheah, Y. K., Halim, S. N. B. A., Seng, H. L. & Tiekink, E. R. T. (2014). *Gold Bull.* **47**, 225–236.

Skrott, Z. & Cvek, B. (2012). *Mini Rev. Med. Chem.* **12**, 1184–1192.

Spek, A. L. (2009). *Acta Cryst.* D**65**, 148–155.

Verma, S. K. & Singh, V. K. (2015). *RSC Adv.* **5**, 53036–53046.

Westrip, S. P. (2010). *J. Appl. Cryst.* **43**, 920–925.

Xu, L. Z., Lin, J. H., Zhang, S. S., Jiao, K. & Jian, F. F. (2001). *Pol. J. Chem*. **75**, 755–757.

Yang, L., Powell, D. R. & Houser, R. P. (2007). *Dalton Trans.* pp. 955–964.

Yeo, C. I., Tan, S. L. & Tiekink, E. R. T. (2016). *Acta Cryst.* E**72**, 1446–1452.

# supporting information

*Acta Cryst.* (2016). E**72**, 1799-1805 [https://doi.org/10.1107/S2056989016017837]

# [*N*,*N*-Bis(2-hydroxyethyl)dithiocarbamato-$\kappa^2 S,S'$]bis(triphenylphosphane-$\kappa P$)copper(I) chloroform monosolvate: crystal structure, Hirshfeld surface analysis and solution NMR measurements

**Sang Loon Tan, Chien Ing Yeo, Peter J. Heard, Geoffrey R. Akien, Nathan R. Halcovitch and Edward R. T. Tiekink**

## Computing details

Data collection: *CrysAlis PRO* (Rigaku Oxford Diffraction, 2015); cell refinement: *CrysAlis PRO* (Rigaku Oxford Diffraction, 2015); data reduction: *CrysAlis PRO* (Rigaku Oxford Diffraction, 2015); program(s) used to solve structure: *SHELXS* (Sheldrick, 2008); program(s) used to refine structure: *SHELXL2014* (Sheldrick, 2015); molecular graphics: *ORTEP-3 for Windows* (Farrugia, 2012), *QMol* (Gans & Shalloway, 2001) and *DIAMOND* (Brandenburg, 2006); software used to prepare material for publication: *publCIF* (Westrip, 2010).

## [*N*,*N*-Bis(2-hydroxyethyl)dithiocarbamato-$\kappa^2 S,S'$]bis(triphenylphosphane-$\kappa P$)copper(I) chloroform monosolvate

*Crystal data*

$[Cu(C_5H_5NO_2S_2)(C_{18}H_{15}P)_2]\cdot CHCl_3$
$M_r$ = 887.71
Triclinic, $P\overline{1}$
$a$ = 10.7271 (2) Å
$b$ = 13.5412 (2) Å
$c$ = 15.9361 (3) Å
$\alpha$ = 67.747 (2)°
$\beta$ = 87.126 (2)°
$\gamma$ = 72.826 (2)°
$V$ = 2041.92 (7) Å$^3$
$Z$ = 2
$F(000)$ = 916
$D_x$ = 1.444 Mg m$^{-3}$
Mo $K\alpha$ radiation, $\lambda$ = 0.71073 Å
Cell parameters from 38605 reflections
$\theta$ = 3.1–30.1°
$\mu$ = 0.95 mm$^{-1}$
$T$ = 100 K
Prism, colourless
0.44 × 0.24 × 0.19 mm

*Data collection*

Rigaku SuperNova, Dual Mo at zero, AtlasS2 diffractometer
Radiation source: micro-focus sealed X-ray tube, SuperNova (Mo) X-ray Source
Mirror monochromator
Detector resolution: 5.2303 pixels mm$^{-1}$
$\omega$ scans
Absorption correction: multi-scan (CrysAlis PRO; Rigaku Oxford Diffraction, 2015)
$T_{min}$ = 0.928, $T_{max}$ = 1.000
78295 measured reflections
11363 independent reflections
10195 reflections with $I > 2\sigma(I)$
$R_{int}$ = 0.029
$\theta_{max}$ = 30.2°, $\theta_{min}$ = 2.4°
$h$ = −14→14
$k$ = −19→18
$l$ = −22→21

*Refinement*

Refinement on $F^2$
Least-squares matrix: full
$R[F^2 > 2\sigma(F^2)] = 0.045$
$wR(F^2) = 0.117$
$S = 1.03$
11363 reflections
478 parameters
0 restraints

Hydrogen site location: mixed
H-atom parameters constrained
$w = 1/[\sigma^2(F_o^2) + (0.0542P)^2 + 3.7972P]$
where $P = (F_o^2 + 2F_c^2)/3$
$(\Delta/\sigma)_{max} = 0.002$
$\Delta\rho_{max} = 1.97$ e Å$^{-3}$
$\Delta\rho_{min} = -1.93$ e Å$^{-3}$

*Special details*

**Geometry**. All esds (except the esd in the dihedral angle between two l.s. planes) are estimated using the full covariance matrix. The cell esds are taken into account individually in the estimation of esds in distances, angles and torsion angles; correlations between esds in cell parameters are only used when they are defined by crystal symmetry. An approximate (isotropic) treatment of cell esds is used for estimating esds involving l.s. planes.

*Fractional atomic coordinates and isotropic or equivalent isotropic displacement parameters (Å$^2$)*

| | *x* | *y* | *z* | $U_{iso}$*/$U_{eq}$ |
|---|---|---|---|---|
| Cu | 0.36192 (2) | 0.77121 (2) | 0.71076 (2) | 0.01300 (7) |
| S1 | 0.19989 (5) | 0.72501 (4) | 0.81318 (3) | 0.01687 (10) |
| S2 | 0.18227 (5) | 0.94266 (4) | 0.66887 (3) | 0.01434 (10) |
| P1 | 0.51698 (5) | 0.80568 (4) | 0.77705 (3) | 0.01311 (10) |
| P2 | 0.40667 (5) | 0.66266 (4) | 0.62988 (3) | 0.01279 (10) |
| O1 | −0.0657 (2) | 1.09492 (18) | 0.86819 (14) | 0.0388 (5) |
| H1O | −0.0221 | 1.1248 | 0.8899 | 0.058* |
| O2 | −0.0552 (2) | 0.89051 (18) | 0.99446 (14) | 0.0379 (5) |
| H2O | −0.0317 | 0.9473 | 0.9646 | 0.057* |
| N1 | 0.00449 (17) | 0.90924 (16) | 0.79337 (12) | 0.0179 (3) |
| C1 | 0.11675 (19) | 0.86434 (16) | 0.76152 (13) | 0.0138 (3) |
| C2 | −0.0662 (2) | 1.02862 (19) | 0.74859 (15) | 0.0222 (4) |
| H2A | −0.1600 | 1.0404 | 0.7600 | 0.027* |
| H2B | −0.0588 | 1.0517 | 0.6822 | 0.027* |
| C3 | −0.0154 (3) | 1.1018 (2) | 0.78121 (17) | 0.0274 (5) |
| H3A | 0.0814 | 1.0761 | 0.7870 | 0.033* |
| H3B | −0.0444 | 1.1802 | 0.7370 | 0.033* |
| C4 | −0.0538 (2) | 0.8356 (2) | 0.86728 (15) | 0.0244 (5) |
| H4A | −0.0415 | 0.7655 | 0.8574 | 0.029* |
| H4B | −0.1491 | 0.8725 | 0.8635 | 0.029* |
| C5 | 0.0018 (2) | 0.8061 (2) | 0.96199 (16) | 0.0276 (5) |
| H5A | −0.0136 | 0.7356 | 1.0035 | 0.033* |
| H5B | 0.0974 | 0.7937 | 0.9613 | 0.033* |
| C11 | 0.4522 (2) | 0.90455 (17) | 0.83239 (13) | 0.0155 (4) |
| C12 | 0.3587 (2) | 0.88068 (19) | 0.89530 (15) | 0.0193 (4) |
| H12 | 0.3316 | 0.8164 | 0.9064 | 0.023* |
| C13 | 0.3054 (2) | 0.9506 (2) | 0.94159 (15) | 0.0223 (4) |
| H13 | 0.2421 | 0.9338 | 0.9842 | 0.027* |
| C14 | 0.3446 (2) | 1.0450 (2) | 0.92569 (16) | 0.0239 (4) |
| H14 | 0.3080 | 1.0928 | 0.9572 | 0.029* |

| | | | | |
|---|---|---|---|---|
| C15 | 0.4374 (3) | 1.0687 (2) | 0.86363 (16) | 0.0264 (5) |
| H15 | 0.4645 | 1.1330 | 0.8528 | 0.032* |
| C16 | 0.4912 (2) | 0.99887 (18) | 0.81703 (15) | 0.0214 (4) |
| H16 | 0.5547 | 1.0158 | 0.7746 | 0.026* |
| C21 | 0.6312 (2) | 0.86383 (16) | 0.69950 (13) | 0.0140 (3) |
| C22 | 0.5816 (2) | 0.96097 (17) | 0.62185 (14) | 0.0186 (4) |
| H22 | 0.4900 | 0.9973 | 0.6120 | 0.022* |
| C23 | 0.6653 (2) | 1.00436 (18) | 0.55932 (15) | 0.0221 (4) |
| H23 | 0.6308 | 1.0706 | 0.5072 | 0.027* |
| C24 | 0.7997 (2) | 0.95133 (19) | 0.57246 (15) | 0.0212 (4) |
| H24 | 0.8568 | 0.9818 | 0.5298 | 0.025* |
| C25 | 0.8497 (2) | 0.85403 (19) | 0.64806 (14) | 0.0196 (4) |
| H25 | 0.9411 | 0.8171 | 0.6568 | 0.024* |
| C26 | 0.7660 (2) | 0.81042 (18) | 0.71115 (14) | 0.0169 (4) |
| H26 | 0.8009 | 0.7436 | 0.7627 | 0.020* |
| C31 | 0.6275 (2) | 0.68849 (17) | 0.86749 (13) | 0.0162 (4) |
| C32 | 0.6884 (2) | 0.70275 (19) | 0.93539 (15) | 0.0218 (4) |
| H32 | 0.6666 | 0.7743 | 0.9389 | 0.026* |
| C33 | 0.7811 (2) | 0.6126 (2) | 0.99804 (16) | 0.0268 (5) |
| H33 | 0.8220 | 0.6228 | 1.0444 | 0.032* |
| C34 | 0.8138 (3) | 0.5084 (2) | 0.99318 (17) | 0.0300 (5) |
| H34 | 0.8781 | 0.4474 | 1.0356 | 0.036* |
| C35 | 0.7531 (3) | 0.4929 (2) | 0.9266 (2) | 0.0347 (6) |
| H35 | 0.7752 | 0.4211 | 0.9236 | 0.042* |
| C36 | 0.6593 (2) | 0.58267 (19) | 0.86396 (18) | 0.0267 (5) |
| H36 | 0.6170 | 0.5716 | 0.8187 | 0.032* |
| C41 | 0.48854 (19) | 0.51623 (16) | 0.69995 (14) | 0.0156 (4) |
| C42 | 0.5952 (2) | 0.45035 (19) | 0.67222 (16) | 0.0220 (4) |
| H42 | 0.6255 | 0.4805 | 0.6136 | 0.026* |
| C43 | 0.6577 (2) | 0.3406 (2) | 0.73001 (18) | 0.0272 (5) |
| H43 | 0.7300 | 0.2961 | 0.7105 | 0.033* |
| C44 | 0.6151 (2) | 0.29608 (19) | 0.81547 (18) | 0.0273 (5) |
| H44 | 0.6593 | 0.2219 | 0.8552 | 0.033* |
| C45 | 0.5079 (3) | 0.3600 (2) | 0.84291 (17) | 0.0273 (5) |
| H45 | 0.4773 | 0.3288 | 0.9012 | 0.033* |
| C46 | 0.4446 (2) | 0.46945 (18) | 0.78592 (16) | 0.0223 (4) |
| H46 | 0.3711 | 0.5127 | 0.8055 | 0.027* |
| C51 | 0.26885 (19) | 0.65508 (16) | 0.57220 (13) | 0.0135 (3) |
| C52 | 0.2709 (2) | 0.55962 (17) | 0.55691 (14) | 0.0169 (4) |
| H52 | 0.3427 | 0.4937 | 0.5812 | 0.020* |
| C53 | 0.1684 (2) | 0.56083 (18) | 0.50627 (15) | 0.0196 (4) |
| H53 | 0.1702 | 0.4958 | 0.4960 | 0.024* |
| C54 | 0.0630 (2) | 0.65717 (19) | 0.47064 (15) | 0.0207 (4) |
| H54 | −0.0067 | 0.6581 | 0.4355 | 0.025* |
| C55 | 0.0595 (2) | 0.75232 (18) | 0.48645 (15) | 0.0192 (4) |
| H55 | −0.0125 | 0.8181 | 0.4622 | 0.023* |
| C56 | 0.16193 (19) | 0.75072 (17) | 0.53791 (14) | 0.0158 (4) |
| H56 | 0.1588 | 0.8151 | 0.5496 | 0.019* |

| | | | | |
|---|---|---|---|---|
| C61 | 0.51483 (19) | 0.69669 (16) | 0.53792 (14) | 0.0150 (4) |
| C62 | 0.4884 (2) | 0.70661 (17) | 0.44993 (14) | 0.0179 (4) |
| H62 | 0.4136 | 0.6900 | 0.4363 | 0.021* |
| C63 | 0.5711 (2) | 0.74078 (18) | 0.38150 (16) | 0.0225 (4) |
| H63 | 0.5526 | 0.7468 | 0.3218 | 0.027* |
| C64 | 0.6801 (2) | 0.7659 (2) | 0.40050 (18) | 0.0266 (5) |
| H64 | 0.7356 | 0.7901 | 0.3538 | 0.032* |
| C65 | 0.7076 (2) | 0.7553 (2) | 0.4883 (2) | 0.0295 (5) |
| H65 | 0.7827 | 0.7716 | 0.5018 | 0.035* |
| C66 | 0.6258 (2) | 0.7211 (2) | 0.55654 (17) | 0.0237 (5) |
| H66 | 0.6454 | 0.7141 | 0.6164 | 0.028* |
| C6 | 0.0552 (3) | 0.4509 (2) | 0.7262 (2) | 0.0354 (6) |
| H6 | 0.0901 | 0.4682 | 0.6646 | 0.042* |
| Cl1 | 0.14649 (11) | 0.31507 (7) | 0.79474 (7) | 0.0593 (3) |
| Cl2 | −0.10822 (9) | 0.46142 (12) | 0.71310 (9) | 0.0740 (4) |
| Cl3 | 0.07466 (6) | 0.55046 (5) | 0.76719 (4) | 0.03169 (13) |

*Atomic displacement parameters (Å²)*

| | $U^{11}$ | $U^{22}$ | $U^{33}$ | $U^{12}$ | $U^{13}$ | $U^{23}$ |
|---|---|---|---|---|---|---|
| Cu | 0.01265 (12) | 0.01232 (11) | 0.01406 (12) | −0.00179 (8) | 0.00184 (8) | −0.00664 (9) |
| S1 | 0.0200 (2) | 0.0124 (2) | 0.0169 (2) | −0.00543 (18) | 0.00520 (18) | −0.00421 (17) |
| S2 | 0.0153 (2) | 0.0118 (2) | 0.0124 (2) | −0.00113 (16) | 0.00266 (16) | −0.00311 (16) |
| P1 | 0.0136 (2) | 0.0124 (2) | 0.0123 (2) | −0.00270 (17) | 0.00066 (17) | −0.00431 (17) |
| P2 | 0.0117 (2) | 0.0117 (2) | 0.0150 (2) | −0.00122 (17) | 0.00111 (17) | −0.00678 (18) |
| O1 | 0.0411 (11) | 0.0450 (12) | 0.0303 (10) | 0.0017 (9) | 0.0000 (8) | −0.0252 (9) |
| O2 | 0.0432 (11) | 0.0421 (11) | 0.0300 (10) | −0.0052 (9) | 0.0066 (8) | −0.0216 (9) |
| N1 | 0.0131 (8) | 0.0227 (9) | 0.0159 (8) | −0.0025 (7) | 0.0033 (6) | −0.0078 (7) |
| C1 | 0.0134 (8) | 0.0163 (9) | 0.0125 (8) | −0.0043 (7) | 0.0015 (7) | −0.0065 (7) |
| C2 | 0.0161 (9) | 0.0255 (11) | 0.0198 (10) | 0.0043 (8) | −0.0011 (8) | −0.0107 (8) |
| C3 | 0.0300 (12) | 0.0218 (11) | 0.0257 (11) | 0.0060 (9) | −0.0041 (9) | −0.0136 (9) |
| C4 | 0.0171 (10) | 0.0363 (13) | 0.0199 (10) | −0.0105 (9) | 0.0076 (8) | −0.0097 (9) |
| C5 | 0.0244 (11) | 0.0366 (13) | 0.0182 (10) | −0.0062 (10) | 0.0046 (8) | −0.0090 (9) |
| C11 | 0.0166 (9) | 0.0161 (9) | 0.0135 (9) | −0.0027 (7) | −0.0002 (7) | −0.0069 (7) |
| C12 | 0.0188 (10) | 0.0219 (10) | 0.0200 (10) | −0.0076 (8) | 0.0039 (8) | −0.0103 (8) |
| C13 | 0.0220 (10) | 0.0269 (11) | 0.0194 (10) | −0.0055 (9) | 0.0044 (8) | −0.0119 (9) |
| C14 | 0.0300 (12) | 0.0234 (11) | 0.0194 (10) | −0.0039 (9) | 0.0027 (9) | −0.0126 (9) |
| C15 | 0.0400 (13) | 0.0209 (10) | 0.0233 (11) | −0.0130 (10) | 0.0068 (10) | −0.0117 (9) |
| C16 | 0.0284 (11) | 0.0194 (10) | 0.0190 (10) | −0.0094 (8) | 0.0055 (8) | −0.0090 (8) |
| C21 | 0.0178 (9) | 0.0127 (8) | 0.0120 (8) | −0.0049 (7) | 0.0004 (7) | −0.0050 (7) |
| C22 | 0.0230 (10) | 0.0134 (9) | 0.0152 (9) | −0.0008 (7) | 0.0012 (8) | −0.0046 (7) |
| C23 | 0.0335 (12) | 0.0135 (9) | 0.0153 (9) | −0.0054 (8) | 0.0040 (8) | −0.0025 (7) |
| C24 | 0.0311 (11) | 0.0200 (10) | 0.0169 (10) | −0.0132 (9) | 0.0084 (8) | −0.0083 (8) |
| C25 | 0.0191 (10) | 0.0245 (10) | 0.0171 (9) | −0.0087 (8) | 0.0029 (8) | −0.0085 (8) |
| C26 | 0.0167 (9) | 0.0187 (9) | 0.0137 (9) | −0.0050 (7) | 0.0002 (7) | −0.0047 (7) |
| C31 | 0.0153 (9) | 0.0159 (9) | 0.0132 (9) | −0.0052 (7) | 0.0003 (7) | −0.0006 (7) |
| C32 | 0.0241 (11) | 0.0226 (10) | 0.0153 (9) | −0.0067 (8) | −0.0009 (8) | −0.0035 (8) |
| C33 | 0.0274 (12) | 0.0311 (12) | 0.0164 (10) | −0.0105 (10) | −0.0048 (8) | −0.0009 (9) |

| | | | | | | |
|---|---|---|---|---|---|---|
| C34 | 0.0268 (12) | 0.0241 (11) | 0.0247 (12) | −0.0076 (9) | −0.0063 (9) | 0.0073 (9) |
| C35 | 0.0373 (14) | 0.0151 (10) | 0.0410 (15) | −0.0023 (10) | −0.0130 (12) | −0.0012 (10) |
| C36 | 0.0292 (12) | 0.0164 (10) | 0.0299 (12) | −0.0050 (9) | −0.0087 (9) | −0.0038 (9) |
| C41 | 0.0146 (9) | 0.0137 (8) | 0.0183 (9) | −0.0020 (7) | −0.0018 (7) | −0.0072 (7) |
| C42 | 0.0199 (10) | 0.0190 (10) | 0.0232 (11) | 0.0006 (8) | 0.0000 (8) | −0.0085 (8) |
| C43 | 0.0213 (11) | 0.0186 (10) | 0.0339 (13) | 0.0049 (8) | −0.0025 (9) | −0.0093 (9) |
| C44 | 0.0259 (11) | 0.0158 (10) | 0.0322 (12) | −0.0018 (8) | −0.0085 (9) | −0.0027 (9) |
| C45 | 0.0308 (12) | 0.0188 (10) | 0.0263 (12) | −0.0079 (9) | 0.0009 (9) | −0.0017 (9) |
| C46 | 0.0218 (10) | 0.0170 (10) | 0.0249 (11) | −0.0042 (8) | 0.0041 (8) | −0.0062 (8) |
| C51 | 0.0126 (8) | 0.0146 (8) | 0.0125 (8) | −0.0039 (7) | 0.0032 (6) | −0.0049 (7) |
| C52 | 0.0156 (9) | 0.0154 (9) | 0.0198 (9) | −0.0023 (7) | 0.0013 (7) | −0.0083 (7) |
| C53 | 0.0198 (10) | 0.0201 (10) | 0.0227 (10) | −0.0072 (8) | 0.0031 (8) | −0.0116 (8) |
| C54 | 0.0156 (9) | 0.0260 (11) | 0.0214 (10) | −0.0068 (8) | 0.0002 (8) | −0.0096 (8) |
| C55 | 0.0138 (9) | 0.0177 (9) | 0.0219 (10) | −0.0013 (7) | −0.0002 (7) | −0.0054 (8) |
| C56 | 0.0143 (9) | 0.0137 (9) | 0.0186 (9) | −0.0030 (7) | 0.0035 (7) | −0.0064 (7) |
| C61 | 0.0131 (8) | 0.0117 (8) | 0.0209 (9) | −0.0018 (7) | 0.0043 (7) | −0.0087 (7) |
| C62 | 0.0174 (9) | 0.0152 (9) | 0.0195 (10) | −0.0038 (7) | 0.0037 (7) | −0.0060 (7) |
| C63 | 0.0245 (11) | 0.0178 (10) | 0.0205 (10) | −0.0044 (8) | 0.0066 (8) | −0.0043 (8) |
| C64 | 0.0239 (11) | 0.0217 (11) | 0.0373 (13) | −0.0098 (9) | 0.0165 (10) | −0.0142 (10) |
| C65 | 0.0198 (11) | 0.0349 (13) | 0.0484 (15) | −0.0146 (10) | 0.0147 (10) | −0.0284 (12) |
| C66 | 0.0177 (10) | 0.0309 (12) | 0.0332 (12) | −0.0088 (9) | 0.0075 (9) | −0.0231 (10) |
| C6 | 0.0351 (14) | 0.0380 (14) | 0.0356 (14) | −0.0135 (12) | −0.0031 (11) | −0.0143 (12) |
| Cl1 | 0.0739 (6) | 0.0376 (4) | 0.0688 (6) | −0.0043 (4) | −0.0159 (5) | −0.0297 (4) |
| Cl2 | 0.0320 (4) | 0.1170 (9) | 0.1089 (9) | −0.0168 (5) | −0.0041 (5) | −0.0847 (8) |
| Cl3 | 0.0340 (3) | 0.0258 (3) | 0.0323 (3) | −0.0095 (2) | −0.0041 (2) | −0.0067 (2) |

*Geometric parameters (Å, º)*

| | | | |
|---|---|---|---|
| Cu—P2 | 2.2380 (5) | C26—H26 | 0.9500 |
| Cu—P1 | 2.2602 (6) | C31—C32 | 1.392 (3) |
| Cu—S1 | 2.3791 (6) | C31—C36 | 1.394 (3) |
| Cu—S2 | 2.4213 (5) | C32—C33 | 1.391 (3) |
| S1—C1 | 1.714 (2) | C32—H32 | 0.9500 |
| S2—C1 | 1.717 (2) | C33—C34 | 1.381 (4) |
| P1—C31 | 1.824 (2) | C33—H33 | 0.9500 |
| P1—C21 | 1.825 (2) | C34—C35 | 1.383 (4) |
| P1—C11 | 1.827 (2) | C34—H34 | 0.9500 |
| P2—C51 | 1.827 (2) | C35—C36 | 1.395 (3) |
| P2—C61 | 1.828 (2) | C35—H35 | 0.9500 |
| P2—C41 | 1.828 (2) | C36—H36 | 0.9500 |
| O1—C3 | 1.442 (3) | C41—C42 | 1.395 (3) |
| O1—H1O | 0.8576 | C41—C46 | 1.398 (3) |
| O2—C5 | 1.397 (3) | C42—C43 | 1.394 (3) |
| O2—H2O | 0.8400 | C42—H42 | 0.9500 |
| N1—C1 | 1.348 (3) | C43—C44 | 1.380 (4) |
| N1—C2 | 1.468 (3) | C43—H43 | 0.9500 |
| N1—C4 | 1.476 (3) | C44—C45 | 1.382 (4) |
| C2—C3 | 1.513 (3) | C44—H44 | 0.9500 |

| | | | |
|---|---|---|---|
| C2—H2A | 0.9900 | C45—C46 | 1.390 (3) |
| C2—H2B | 0.9900 | C45—H45 | 0.9500 |
| C3—H3A | 0.9900 | C46—H46 | 0.9500 |
| C3—H3B | 0.9900 | C51—C56 | 1.393 (3) |
| C4—C5 | 1.512 (3) | C51—C52 | 1.397 (3) |
| C4—H4A | 0.9900 | C52—C53 | 1.389 (3) |
| C4—H4B | 0.9900 | C52—H52 | 0.9500 |
| C5—H5A | 0.9900 | C53—C54 | 1.391 (3) |
| C5—H5B | 0.9900 | C53—H53 | 0.9500 |
| C11—C16 | 1.391 (3) | C54—C55 | 1.393 (3) |
| C11—C12 | 1.400 (3) | C54—H54 | 0.9500 |
| C12—C13 | 1.391 (3) | C55—C56 | 1.394 (3) |
| C12—H12 | 0.9500 | C55—H55 | 0.9500 |
| C13—C14 | 1.391 (3) | C56—H56 | 0.9500 |
| C13—H13 | 0.9500 | C61—C62 | 1.393 (3) |
| C14—C15 | 1.386 (3) | C61—C66 | 1.398 (3) |
| C14—H14 | 0.9500 | C62—C63 | 1.397 (3) |
| C15—C16 | 1.395 (3) | C62—H62 | 0.9500 |
| C15—H15 | 0.9500 | C63—C64 | 1.387 (3) |
| C16—H16 | 0.9500 | C63—H63 | 0.9500 |
| C21—C26 | 1.399 (3) | C64—C65 | 1.390 (4) |
| C21—C22 | 1.402 (3) | C64—H64 | 0.9500 |
| C22—C23 | 1.386 (3) | C65—C66 | 1.389 (3) |
| C22—H22 | 0.9500 | C65—H65 | 0.9500 |
| C23—C24 | 1.394 (3) | C66—H66 | 0.9500 |
| C23—H23 | 0.9500 | C6—Cl2 | 1.733 (3) |
| C24—C25 | 1.386 (3) | C6—Cl1 | 1.748 (3) |
| C24—H24 | 0.9500 | C6—Cl3 | 1.771 (3) |
| C25—C26 | 1.392 (3) | C6—H6 | 1.0000 |
| C25—H25 | 0.9500 | | |

| | | | |
|---|---|---|---|
| P2—Cu—P1 | 123.65 (2) | C24—C25—H25 | 120.0 |
| P2—Cu—S1 | 109.81 (2) | C26—C25—H25 | 120.0 |
| P1—Cu—S1 | 110.96 (2) | C25—C26—C21 | 120.80 (19) |
| P2—Cu—S2 | 123.17 (2) | C25—C26—H26 | 119.6 |
| P1—Cu—S2 | 103.74 (2) | C21—C26—H26 | 119.6 |
| S1—Cu—S2 | 75.264 (18) | C32—C31—C36 | 119.2 (2) |
| C1—S1—Cu | 84.12 (7) | C32—C31—P1 | 122.25 (16) |
| C1—S2—Cu | 82.75 (7) | C36—C31—P1 | 118.39 (16) |
| C31—P1—C21 | 101.95 (9) | C33—C32—C31 | 120.2 (2) |
| C31—P1—C11 | 101.78 (9) | C33—C32—H32 | 119.9 |
| C21—P1—C11 | 104.44 (9) | C31—C32—H32 | 119.9 |
| C31—P1—Cu | 118.06 (7) | C34—C33—C32 | 120.3 (2) |
| C21—P1—Cu | 114.57 (7) | C34—C33—H33 | 119.9 |
| C11—P1—Cu | 114.16 (7) | C32—C33—H33 | 119.9 |
| C51—P2—C61 | 102.10 (9) | C33—C34—C35 | 120.0 (2) |
| C51—P2—C41 | 103.13 (9) | C33—C34—H34 | 120.0 |
| C61—P2—C41 | 103.77 (9) | C35—C34—H34 | 120.0 |

| | | | |
|---|---|---|---|
| C51—P2—Cu | 117.50 (6) | C34—C35—C36 | 120.0 (2) |
| C61—P2—Cu | 116.28 (7) | C34—C35—H35 | 120.0 |
| C41—P2—Cu | 112.27 (7) | C36—C35—H35 | 120.0 |
| C3—O1—H1O | 105.7 | C31—C36—C35 | 120.2 (2) |
| C5—O2—H2O | 109.4 | C31—C36—H36 | 119.9 |
| C1—N1—C2 | 120.12 (18) | C35—C36—H36 | 119.9 |
| C1—N1—C4 | 119.48 (18) | C42—C41—C46 | 118.73 (19) |
| C2—N1—C4 | 120.09 (18) | C42—C41—P2 | 122.71 (17) |
| N1—C1—S1 | 120.50 (15) | C46—C41—P2 | 118.53 (16) |
| N1—C1—S2 | 122.12 (15) | C41—C42—C43 | 120.4 (2) |
| S1—C1—S2 | 117.38 (11) | C41—C42—H42 | 119.8 |
| N1—C2—C3 | 113.01 (18) | C43—C42—H42 | 119.8 |
| N1—C2—H2A | 109.0 | C44—C43—C42 | 120.3 (2) |
| C3—C2—H2A | 109.0 | C44—C43—H43 | 119.8 |
| N1—C2—H2B | 109.0 | C42—C43—H43 | 119.8 |
| C3—C2—H2B | 109.0 | C43—C44—C45 | 119.7 (2) |
| H2A—C2—H2B | 107.8 | C43—C44—H44 | 120.1 |
| O1—C3—C2 | 108.3 (2) | C45—C44—H44 | 120.1 |
| O1—C3—H3A | 110.0 | C44—C45—C46 | 120.5 (2) |
| C2—C3—H3A | 110.0 | C44—C45—H45 | 119.7 |
| O1—C3—H3B | 110.0 | C46—C45—H45 | 119.7 |
| C2—C3—H3B | 110.0 | C45—C46—C41 | 120.3 (2) |
| H3A—C3—H3B | 108.4 | C45—C46—H46 | 119.8 |
| N1—C4—C5 | 114.9 (2) | C41—C46—H46 | 119.8 |
| N1—C4—H4A | 108.5 | C56—C51—C52 | 119.51 (18) |
| C5—C4—H4A | 108.5 | C56—C51—P2 | 118.08 (15) |
| N1—C4—H4B | 108.5 | C52—C51—P2 | 122.29 (15) |
| C5—C4—H4B | 108.5 | C53—C52—C51 | 120.22 (19) |
| H4A—C4—H4B | 107.5 | C53—C52—H52 | 119.9 |
| O2—C5—C4 | 111.6 (2) | C51—C52—H52 | 119.9 |
| O2—C5—H5A | 109.3 | C52—C53—C54 | 120.1 (2) |
| C4—C5—H5A | 109.3 | C52—C53—H53 | 119.9 |
| O2—C5—H5B | 109.3 | C54—C53—H53 | 119.9 |
| C4—C5—H5B | 109.3 | C53—C54—C55 | 120.0 (2) |
| H5A—C5—H5B | 108.0 | C53—C54—H54 | 120.0 |
| C16—C11—C12 | 119.11 (19) | C55—C54—H54 | 120.0 |
| C16—C11—P1 | 124.41 (16) | C54—C55—C56 | 119.85 (19) |
| C12—C11—P1 | 116.47 (16) | C54—C55—H55 | 120.1 |
| C13—C12—C11 | 120.4 (2) | C56—C55—H55 | 120.1 |
| C13—C12—H12 | 119.8 | C51—C56—C55 | 120.29 (19) |
| C11—C12—H12 | 119.8 | C51—C56—H56 | 119.9 |
| C14—C13—C12 | 120.2 (2) | C55—C56—H56 | 119.9 |
| C14—C13—H13 | 119.9 | C62—C61—C66 | 118.8 (2) |
| C12—C13—H13 | 119.9 | C62—C61—P2 | 123.81 (16) |
| C15—C14—C13 | 119.6 (2) | C66—C61—P2 | 117.29 (16) |
| C15—C14—H14 | 120.2 | C61—C62—C63 | 120.5 (2) |
| C13—C14—H14 | 120.2 | C61—C62—H62 | 119.7 |
| C14—C15—C16 | 120.4 (2) | C63—C62—H62 | 119.7 |

| | | | |
|---|---|---|---|
| C14—C15—H15 | 119.8 | C64—C63—C62 | 120.2 (2) |
| C16—C15—H15 | 119.8 | C64—C63—H63 | 119.9 |
| C11—C16—C15 | 120.3 (2) | C62—C63—H63 | 119.9 |
| C11—C16—H16 | 119.9 | C63—C64—C65 | 119.6 (2) |
| C15—C16—H16 | 119.9 | C63—C64—H64 | 120.2 |
| C26—C21—C22 | 118.63 (19) | C65—C64—H64 | 120.2 |
| C26—C21—P1 | 122.28 (15) | C66—C65—C64 | 120.3 (2) |
| C22—C21—P1 | 118.91 (16) | C66—C65—H65 | 119.8 |
| C23—C22—C21 | 120.4 (2) | C64—C65—H65 | 119.8 |
| C23—C22—H22 | 119.8 | C65—C66—C61 | 120.6 (2) |
| C21—C22—H22 | 119.8 | C65—C66—H66 | 119.7 |
| C22—C23—C24 | 120.4 (2) | C61—C66—H66 | 119.7 |
| C22—C23—H23 | 119.8 | Cl2—C6—Cl1 | 111.63 (17) |
| C24—C23—H23 | 119.8 | Cl2—C6—Cl3 | 111.63 (17) |
| C25—C24—C23 | 119.7 (2) | Cl1—C6—Cl3 | 111.60 (15) |
| C25—C24—H24 | 120.1 | Cl2—C6—H6 | 107.2 |
| C23—C24—H24 | 120.1 | Cl1—C6—H6 | 107.2 |
| C24—C25—C26 | 120.0 (2) | Cl3—C6—H6 | 107.2 |

| | | | |
|---|---|---|---|
| C2—N1—C1—S1 | −179.88 (15) | P1—C31—C32—C33 | −174.02 (18) |
| C4—N1—C1—S1 | −6.2 (3) | C31—C32—C33—C34 | 0.3 (4) |
| C2—N1—C1—S2 | 0.1 (3) | C32—C33—C34—C35 | −0.9 (4) |
| C4—N1—C1—S2 | 173.79 (16) | C33—C34—C35—C36 | 0.4 (4) |
| Cu—S1—C1—N1 | −173.40 (17) | C32—C31—C36—C35 | −1.3 (4) |
| Cu—S1—C1—S2 | 6.57 (10) | P1—C31—C36—C35 | 173.7 (2) |
| Cu—S2—C1—N1 | 173.49 (17) | C34—C35—C36—C31 | 0.7 (4) |
| Cu—S2—C1—S1 | −6.48 (10) | C51—P2—C41—C42 | 96.01 (19) |
| C1—N1—C2—C3 | −84.6 (2) | C61—P2—C41—C42 | −10.2 (2) |
| C4—N1—C2—C3 | 101.8 (2) | Cu—P2—C41—C42 | −136.55 (17) |
| N1—C2—C3—O1 | −77.9 (2) | C51—P2—C41—C46 | −85.86 (18) |
| C1—N1—C4—C5 | 83.8 (3) | C61—P2—C41—C46 | 167.95 (17) |
| C2—N1—C4—C5 | −102.5 (2) | Cu—P2—C41—C46 | 41.58 (19) |
| N1—C4—C5—O2 | 82.1 (3) | C46—C41—C42—C43 | −1.0 (3) |
| C31—P1—C11—C16 | 103.55 (19) | P2—C41—C42—C43 | 177.13 (18) |
| C21—P1—C11—C16 | −2.2 (2) | C41—C42—C43—C44 | −0.3 (4) |
| Cu—P1—C11—C16 | −128.12 (17) | C42—C43—C44—C45 | 1.6 (4) |
| C31—P1—C11—C12 | −75.31 (18) | C43—C44—C45—C46 | −1.4 (4) |
| C21—P1—C11—C12 | 178.89 (16) | C44—C45—C46—C41 | 0.1 (4) |
| Cu—P1—C11—C12 | 53.01 (17) | C42—C41—C46—C45 | 1.1 (3) |
| C16—C11—C12—C13 | 0.2 (3) | P2—C41—C46—C45 | −177.09 (19) |
| P1—C11—C12—C13 | 179.10 (17) | C61—P2—C51—C56 | −94.07 (16) |
| C11—C12—C13—C14 | 0.0 (3) | C41—P2—C51—C56 | 158.48 (16) |
| C12—C13—C14—C15 | −0.2 (4) | Cu—P2—C51—C56 | 34.40 (18) |
| C13—C14—C15—C16 | 0.2 (4) | C61—P2—C51—C52 | 82.03 (18) |
| C12—C11—C16—C15 | −0.2 (3) | C41—P2—C51—C52 | −25.42 (19) |
| P1—C11—C16—C15 | −179.03 (18) | Cu—P2—C51—C52 | −149.50 (15) |
| C14—C15—C16—C11 | 0.0 (4) | C56—C51—C52—C53 | 1.3 (3) |
| C31—P1—C21—C26 | 8.01 (19) | P2—C51—C52—C53 | −174.71 (16) |

| | | | |
|---|---|---|---|
| C11—P1—C21—C26 | 113.67 (18) | C51—C52—C53—C54 | −0.1 (3) |
| Cu—P1—C21—C26 | −120.71 (16) | C52—C53—C54—C55 | −0.6 (3) |
| C31—P1—C21—C22 | −176.85 (16) | C53—C54—C55—C56 | 0.1 (3) |
| C11—P1—C21—C22 | −71.19 (18) | C52—C51—C56—C55 | −1.9 (3) |
| Cu—P1—C21—C22 | 54.43 (17) | P2—C51—C56—C55 | 174.34 (16) |
| C26—C21—C22—C23 | −1.6 (3) | C54—C55—C56—C51 | 1.2 (3) |
| P1—C21—C22—C23 | −176.94 (17) | C51—P2—C61—C62 | −2.56 (19) |
| C21—C22—C23—C24 | 0.6 (3) | C41—P2—C61—C62 | 104.40 (18) |
| C22—C23—C24—C25 | 0.6 (3) | Cu—P2—C61—C62 | −131.80 (16) |
| C23—C24—C25—C26 | −0.9 (3) | C51—P2—C61—C66 | 173.12 (17) |
| C24—C25—C26—C21 | −0.2 (3) | C41—P2—C61—C66 | −79.91 (18) |
| C22—C21—C26—C25 | 1.4 (3) | Cu—P2—C61—C66 | 43.89 (18) |
| P1—C21—C26—C25 | 176.57 (16) | C66—C61—C62—C63 | −0.3 (3) |
| C21—P1—C31—C32 | 79.67 (19) | P2—C61—C62—C63 | 175.35 (16) |
| C11—P1—C31—C32 | −28.1 (2) | C61—C62—C63—C64 | −0.4 (3) |
| Cu—P1—C31—C32 | −153.85 (16) | C62—C63—C64—C65 | 0.9 (3) |
| C21—P1—C31—C36 | −95.22 (19) | C63—C64—C65—C66 | −0.7 (4) |
| C11—P1—C31—C36 | 157.05 (19) | C64—C65—C66—C61 | 0.0 (4) |
| Cu—P1—C31—C36 | 31.3 (2) | C62—C61—C66—C65 | 0.5 (3) |
| C36—C31—C32—C33 | 0.8 (3) | P2—C61—C66—C65 | −175.44 (18) |

*Hydrogen-bond geometry (Å, º)*

*Cg*1 is the ring centroid of (C51–C56).

| *D*—H···*A* | *D*—H | H···*A* | *D*···*A* | *D*—H···*A* |
|---|---|---|---|---|
| O2—H2*O*···O1 | 0.84 | 1.95 | 2.710 (3) | 150 |
| O1—H1*O*···O2$^{i}$ | 0.86 | 1.97 | 2.697 (3) | 142 |
| C6—Cl3···*Cg*1 | 1.77 (1) | 3.81 (1) | 3.798 (3) | 76 (1) |

Symmetry code: (i) −*x*, −*y*+2, −*z*+2.